Available online at www.sciencedirect.com

ScienceDirect

Geochimica et Cosmochimica Acta 259 (2019) 37–52

Geochimica et Cosmochimica Acta

www.elsevier.com/locate/gca

Calcium isotope fractionation during crustal melting and magma differentiation: Granitoid and mineral-pair perspectives

Yang Wang (王阳) [a], Yongsheng He [a,*], Hongjie Wu [a], Chuanwei Zhu [a], Shichun Huang [b], Jian Huang [c]

[a] State Key Laboratory of Geological Processes and Mineral Resources, China University of Geosciences, Beijing 100083, China
[b] Department of Geoscience, University of Nevada, Las Vegas, NV 89154, United States
[c] CAS Key Laboratory of Crust-Mantle Materials and Environments, University of Science and Technology of China, Hefei, Anhui 230026, China

Received 20 November 2018; accepted in revised form 22 May 2019; Available online 8 June 2019

Abstract

In order to investigate Ca isotope fractionation during crustal melting and magma differentiation, we report high-precision Ca isotopic data of 17 well-characterized granitoids from the Dabie orogen, China, and 22 mineral separates from two representative granitoids and nine local eclogites and garnet peridotites. Hornblende and plagioclase pairs have nearly constant $\Delta^{44/42}Ca_{hbl-plg}$, ranging from $+0.09 \pm 0.04$ (in 2SE if not specified) to $+0.12 \pm 0.03$, which likely reflects equilibrium inter-mineral isotope fractionation at 660–760 °C according to the plagioclase–hornblende geothermometry. $\Delta^{44/42}Ca_{grt-cpx}$ of eclogites and garnet peridotites range from $+0.06 \pm 0.03$ to $+0.38 \pm 0.04$, consistent with a stronger Ca—O bond in garnet than clinopyroxene. $A_{grt-cpx}$ ($A_{grt-cpx} = \Delta^{44/42}Ca_{grt-cpx} \times T^2/10^6$, T in Kelvin), representative of inter-mineral isotope fractionation corrected for temperature effect, decreases with increasing jadeite proportion in clinopyroxene, indicating a compositional control on equilibrium inter-mineral isotope fractionation.

Eight I-type non-adakitic granitoids with CaO contents ranging from 1.59 wt.% to 6.96 wt.% have homogeneous Ca isotopic compositions with an average $\delta^{44/42}Ca$ of $+0.37 \pm 0.03$ (2SD, N = 8), identical to the mean value of the local basement ($+0.36 \pm 0.06$, 2SD), indicating insignificant Ca isotope fractionation during crustal melting and magma differentiation at low pressures (e.g., without a role of garnet). According to the negligible isotope fractionation between hornblende and plagioclase ($\Delta^{44/42}Ca_{hbl-plg} = (+0.10 \pm 0.02) \times 10^6/T^2$) at the liquidus temperatures, the Ca isotope fractionations between melt and hornblende, plagioclase are very small. Nine low-Mg adakitic granitoids have $\delta^{44/42}Ca$ ranging from $+0.24 \pm 0.02$ to $+0.38 \pm 0.02$. Given their low chemical index of alteration (<51), limited CaO variation (1.86–3.07 wt.%), and mineral assemblage similar to that of non-adakitic granitoids, $\delta^{44/42}Ca$ variation in low-Mg adakitic samples cannot be explained by either weathering or fractional crystallization. $\delta^{44/42}Ca$ is negatively correlated with $(Dy/Yb)_N$, which most likely reflects the role of residual jadeite-rich clinopyroxene and garnet. Model calculation suggests that the lowest $\delta^{44/42}Ca$ adakitic sample requires 30% garnet and 70% clinopyroxene (with 28% jadeite) in its residue, consistent with a local crust thickness greater than 50 km. Our results indicate that Ca isotopes can be used as a potential tool to constrain the magma generation depth, because garnet and jadeite-rich clinopyroxene tend to be rich in heavier Ca isotopes. Combined with literature data, the upper continent crust $\delta^{44/42}Ca$ is estimated to be $+0.35 \pm 0.05$ (2SE, 95% c.i.).

Keywords: Calcium isotopes; Isotope fractionation; Granitoids; Crustal melting and differentiation; Garnet and jadeite effect

* Corresponding author.
E-mail address: heys@cugb.edu.cn (Y. He).

https://doi.org/10.1016/j.gca.2019.05.030
0016-7037/

1. INTRODUCTION

Substantial stable Ca isotopic variations have been observed among terrestrial igneous rocks, with $\delta^{44/42}$Ca ($\delta^{44/42}\text{Ca}(‰) = \left[\left(^{44}Ca/^{42}Ca\right)_{sample}/\left(^{44}Ca/^{42}Ca\right)_{SRM915a} - 1\right] \times 1000$) ranging from −0.04 to +0.80 (e.g., Huang et al., 2010; Fantle and Tipper, 2014; Valdes et al., 2014; Kang et al., 2016; He et al., 2017a; Kang et al., 2017; Zhao et al., 2017; see Fig. 1 of Zhang et al. (2018) for a summary of $\delta^{44/40}$Ca), which is 15 times larger than the current analytical uncertainty (ca. 0.03–0.05, in 2SD, e.g., Lehn and Jacobson, 2015; He et al., 2017a), showing great potential in tracing source heterogeneity and magmatic processes.

Calcium isotope fractionation during magmatic processes, however, remains poorly understood. The observed $\delta^{44/42}$Ca range in igneous rocks has been attributed to recycling of surface materials to magma sources (Huang et al., 2011; He et al., 2017a; Liu et al., 2017a), isotope fractionation during partial melting and magma differentiation (Huang et al., 2011; Valdes et al., 2014; He et al., 2017a; Kang et al., 2017), or kinetic processes (Zhao et al., 2017). A recent compilation of published high precision data of terrestrial standard samples reveals that samples with light Ca isotopic compositions tend to have high $(Dy/Yb)_N$ (He et al., 2017a). Since garnet may be enriched in heavier Ca isotopes than its co-existing clinopyroxene (Magna et al., 2015), garnet-involved magma processes can possibly lead to significant Ca isotopic variations (He et al., 2017a). Detailed works are required to study Ca isotope fractionation between garnet and co-existing minerals and during garnet-involved magma processes, because (i) Ca isotopic data of garnet and co-existing minerals are still lacking, and (ii) reported standard samples are from different localities with quite variable petrogenesis.

Adakitic rocks are useful in investigating the role of garnet in fractionating Ca isotopes, because they are formed from partial melting of basaltic rocks with garnet-pyroxene-dominant residua. They are identified by their distinct chemical features, e.g., high Sr/Y (>40), $(La/Yb)_N$ (>20) and low Y (≤18 μg/g) and Yb (≤1.9 μg/g) contents, which are interpreted as a result of partial melting of subducted oceanic crust (Defant and Drummond, 1990) or thickened/delaminated lower continental crust (e.g., Atherton and Petford, 1993; Wang et al., 2007; Huang et al., 2008; He et al., 2011). Nevertheless, adakitic rocks related to partial melting of subducted oceanic crust and delaminated lower continental crust generally can be modified by melt-mantle interaction to variable extent when penetrating the ambient mantle in route to the surface (Defant and Drummond, 1990; Rapp et al., 1999; Huang et al., 2008), which may complicate Ca isotope fractionation during the formation of adakitic rocks. Some adakitic rocks with low Mg#, MgO, Cr and Ni content (low-Mg adakitic rocks) are thought to have not interacted with the upper mantle and represent pristine partial melts of a thickened lower crust leaving garnet-pyroxene-dominant residua at depth >50 km (e.g., Atherton and Petford, 1993; Wang et al., 2007; He et al., 2011). Combined with their variable amounts of residual garnet, low-Mg adakitic rocks are thus the best for constraining the role of garnet in Ca isotope fractionation. Although high Sr/Y magmas in continental settings can be produced in many ways other than partial melting of basaltic sources with eclogitic residua such as fractional crystallization or derivation from a high Sr/Y sources (Moyen, 2009), low-Mg adakitic rocks in some locations, e.g., the Dabie orogen, have been previously documented as partial melts of a thickened lower crust at depth >50 km (Wang et al., 2007; He et al., 2011).

Zhang et al. (2018) reported no-measurable Ca isotope fractionation during crystal fractionation of basaltic magma, and inferred no-measurable Ca isotope fractionation during partial melting of spinel peridotite. Here, to investigate Ca isotope fractionation in intermediate to felsic rocks during crustal melting and magma differentiation with or without garnet involved, we report high-precision Ca isotopic compositions of nine early Cretaceous low-Mg adakitic granitoids from the Dabie orogen in central China, complemented by eight non-adakitic I-type granitoids that are derived from shallower depths (<40 km) without garnet involved in their petrogenesis (Wang et al., 2007; He et al., 2011). To facilitate the explanation of whole rock data, key minerals involved are also measured, including hornblende and plagioclase as major Ca-bearing minerals in Dabie granitoids and garnet and clinopyroxene from Dabie eclogites and Sulu garnet peridotites that are expected to be representative of residual minerals for low-Mg adakitic granitoids. Our results show that (i) non-adakitic granitoids have homogeneous Ca isotopic compositions similar to that of the local basement, indicating insignificant fractionation during crustal melting and/or magma differentiation without garnet and jadeite-rich clinopyroxene involved; (ii) $\delta^{44/42}$Ca of low-Mg adakitic granitoids are negatively correlated with $(Dy/Yb)_N$, which is most likely resulted from the role of residual garnet and jadeite-rich clinopyroxene on Ca isotope fractionation during crustal melting.

2. SAMPLE DESCRIPTION

Post-collisional granitoids extensively and intensively intruded the Dabie orogen in the early Cretaceous (e.g., Wang et al., 2007; He et al., 2011). The early stage granitoids emplaced at 143–130 Ma were low-Mg adakitic, with positively inter-correlated high Sr/Y (31.9–333.0), $(La/Yb)_N$ (20.2–288.3) and $(Dy/Yb)_N$ (1.0–3.2) ratios (Wang et al., 2007; He et al., 2011 and references therein). The trace elemental features of the low-Mg adakitic granitoids indicate plagioclase-poor and garnet-rich residua, suggesting derivation from thickened (>50 km) mafic lower continental crust (LCC) (He et al., 2011). Such a garnet + clinopyroxene dominant residual assemblage is supported by garnet, omphacite and rutile inclusions found in magmatic zircons of Dabie low-Mg adakitic granitoids (Chang et al., 2014). Liquidus experiments indicate partial melting most likely occurred at $T \geq 1075$ °C and $P \geq 2$ GPa and with initial melt H_2O of ~6 wt.% (Xiao and Clemens, 2007). In contrast, granitoids emplaced after 130 Ma in the orogen have non-adakitic features with

Sr/Y, $(La/Yb)_N$ and $(Dy/Yb)_N$ substantially lower than low-Mg adakitic granitoids (Wang et al., 2007; He et al., 2011). Therefore, Dabie non-adakitic granitoids were likely derived from a shallower (<40 km) crust with garnet-poor and plagioclase- and clinopyroxene-rich residua (He et al., 2011 and references therein). This compositional transition in granitoids, simultaneous to the emplacement of high-Mg adakitic rocks at ca. 130 Ma (Huang et al., 2008), reflects delamination of the pre-existing thickened LCC at ca. 130 Ma (Wang et al., 2007; He et al., 2011). Dabie non-adakitic granitoids have highly variable compositions, reflecting melting of various lithologies in the orogenic crust post delamination due to mantle upwelling. Most non-adakitic granitoids are I-type (Wang et al., 2007), and a few S-type and A-type granitoids are also outcropped (e.g., Wang et al., 2007; Chen et al., 2017). To study Ca isotope fractionation during magmatic processes, only I-type granitoids were measured in this study to avoid potential influence by supracrustal material recycling.

Eight non-adakitic and nine low-Mg adakitic Dabie granitoids (Fig. 1) were measured in this study for Ca isotopic compositions. Their petrology, elemental compositions and Sr–Nd–Pb–Mg–Fe isotopic compositions have been well characterized (Wang et al., 2007; Liu et al., 2010; He et al., 2011; He et al., 2013; He et al., 2017b; Wu et al., 2017). Non-adakitic granitoids samples in this study are metaluminous to weakly peraluminous with A/CNK ($Al_2O_3/(CaO + Na_2O + K_2O)$ in a mole ratio) ranging from 0.71 to 1.01, typical of I-type granitoids (He et al., 2011). The $(Dy/Yb)_N$ of non-adakitic granitoids ranges from 1.04 to 1.75, with an average of 1.43, similar to the mean lower continental crust (1.38, Rudnick and Gao, 2003). Garnet should thus be absent in residua of these non-adakitic granitoids (He et al., 2011). All granitoids in this study contain various amounts of quartz, plagioclase, alkali-feldspar, biotite and minor accessory minerals (Fig. S1; Wu et al., 2017). Hornblende is observed in all samples except for low-Mg adakitic granitoids EGB-2 and 07LS-5. About 10% clinopyroxene is observed in 07FJS-2. As major Ca carriers, coexisting hornblende and plagioclase of low-Mg adakitic sample 07LD-2 and non-adakitic sample 07YX-3 were analyzed for their Ca isotopic compositions.

To constrain isotope fractionation between garnet and clinopyroxene, garnet and clinopyroxene separates from eclogites (Bixiling, Shuanghe and Hong'an) and garnet peridotites (Zhimafang) from the Dabie-Sulu orogen were analyzed for Ca isotopic compositions. Studied Dabie eclogites are unaltered and occur as tectonic block, layers or lenses in ultrahigh-pressure gneisses. Their estimated Fe–Mg exchange temperatures between garnet and clinopyroxene range from 479 to 700 °C, and their detailed petrological and geochemical features are reported in previous work (Li et al., 2011; Li et al., 2016 and references therein). Zhimafang garnet peridotites represent exhumed mantle wedge fragments. They are metamorphosed at high pressure and temperature (e.g., Liu et al., 2015; Wang et al., 2017c).

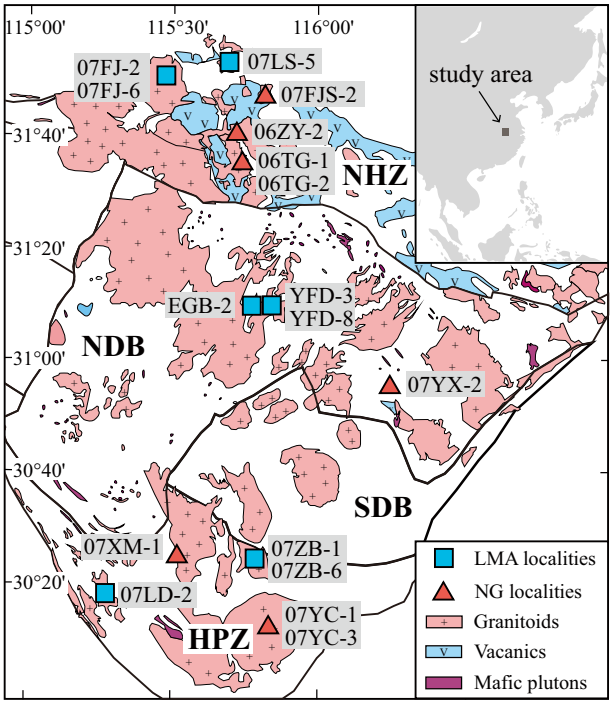

Fig. 1. Generalized geological map of the Dabie orogen modified after He et al. (2011) and references therein. NHZ, NDB, SDB and HPZ represent the North Huaiyang Zone, the North Dabie Zone, the South Dabie Zone, and the Susong High Pressure Metamorphic Zone, respectively. LMA and NG are abbreviations of low-Mg adakitic granitoids and non-adakitic granitoids, respectively.

3. ANALYTICAL METHODS

Bulk rocks were first broken using steel jaw crushers, and fine crushed to a size of ~0.25 mm. Then they were processed through magnetic and density separation. The mineral separates were carefully handpicked from preliminarily purified mineral splits under a binocular microscope to ensure purity and absence of alteration. All mineral separates were then cleaned in Milli-Q water in an ultrasonic bath for 10 minutes twice.

Calcium isotopic analysis was conducted at the Isotope Geochemistry Laboratory, China University of Geosciences, Beijing, following the procedures detailed in He et al. (2017a). About 3–20 mg powders or 2–6 mg minerals (containing at least 100 μg Ca) were dissolved using 1.5 ml concentrated HF + 0.5 ml concentrated HNO_3 at 100 °C for 72 hours. Then the solutions were dried down and evaporated with 0.5 ml concentrated HCl at 120 °C three times to break down CaF_2. Finally, the samples were dissolved in 0.5 ml 2.5 N HCl. An aliquot containing 30–50 μg of Ca was transferred into a pre-cleaned 6 ml Teflon beaker and mixed with a ^{43}Ca–^{48}Ca double-spike to have $^{48}Ca/^{40}Ca$ of ca. 0.1145. Calcium was purified using ca. 1.4 ml AG50W-X12 resin (200–400 mesh) in a 2.5 N HCl medium. The same column chemistry was repeated twice to ensure purity. The whole procedure Ca yield after two column chemistry was about 90%, and blank is typically less than 20 ng, ≤0.4% of the sample Ca processed. The purified Ca was dried down with two drops of concentrated HNO_3 prior to isotopic measurement.

Calcium isotopic ratios were determined on a Triton Plus thermal ionization mass-spectrometer (TIMS) using a Re double filament assemblage. About 5 μg Ca was loaded using 2 μl 3% HNO_3. Ionization and evaporation currents were set to ~3300 mA and ~150 mA, respectively, with a ^{40}Ca signal of ~20 V. Our TIMS was equipped with customized Faraday cups L5 for ^{40}Ca and H4 for ^{48}Ca respectively, which allow static measurement of masses from 40 to 48 u. The isobaric interference of ^{40}K was monitored using ^{41}K which is negligible (<6 μmol/mol on ^{40}Ca). A routine measurement consists of 120 cycles with an integration time of 16.776 s. Data reduction was conducted offline using an Excel Macro program established by He et al. (2017a). Calcium isotopic compositions are reported relative to NIST SRM 915a using δ notation:

$$\delta^{44/i}Ca(‰) = \left(\frac{^{44}Ca/^{i}Ca_{sample}}{^{44}Ca/^{i}Ca_{SRM915a}} - 1\right) \times 1000 \quad (1)$$

where i is 40 or 42. ^{40}Ca is one of two daughter products from the branched decay of ^{40}K. Thus, radiogenic ^{40}Ca contribution could be significant in ancient rocks with high K_2O/CaO or due to source inheritance. Given the high K_2O/CaO ratios in granitoids (e.g., ranging from 0.40 to 3.66 in this study), measured $\delta^{44/40}Ca$ may reflect the combined effect of ^{40}K decaying and mass-dependent isotope fractionation. Therefore, we use $\delta^{44/42}Ca$ in this paper. The radiogenic ^{40}Ca excess relative to NIST SRM 915a ($\varepsilon^{40/44}Ca$) can be calculated based on the equation:

$$\varepsilon^{40/44}Ca = [(\delta^{44/42}Ca \times 2.0483) - \delta^{44/40}Ca] \times 10 \quad (2)$$

where the coefficient of 2.0483 represents the slope of the exponential mass-dependent fractionation (Farkaš et al., 2011; Huang et al., 2012).

Each sample was loaded on four to six filaments, and each filament was measured 1–2 times independently. In this study, two standard error of the mean was reported as analytical uncertainty if not specified. The long-term precision (2SD) of $\delta^{44/42}Ca$ and $\varepsilon^{40/44}Ca$ are typically ±0.03 and ±1.0 respectively, if each sample was analyzed eight times (He et al., 2017a). Measurements of NIST SRM915b and Atlantic seawater during the course of this study (2015.11.11–2019.4.6) yield average $\delta^{44/42}Ca$ of +0.35 ± 0.01 (2SE, N = 73) and +0.90 ± 0.01 (2SE, N = 66) respectively (Table 1), consistent with published values within errors (e.g., Huang et al., 2010; Lehn and Jacobson, 2015; He et al., 2017a; Table 1).

4. RESULTS

Calcium isotopic data of whole rocks and mineral separates are reported in Tables 1 and 2 respectively, and whole rock data are shown in Fig. 2. Hornblendes (hbl) from 07LD-2 and 07YX-3 have identical $\delta^{44/42}Ca$ (+0.43 ± 0.02 and +0.44 ± 0.03), higher than their coexisting plagioclases (plg) (+0.32 ± 0.02 and +0.35 ± 0.03), with a $\Delta^{44/42}Ca_{hbl-plg}$ ($\Delta^{44/42}Ca_{hbl-plg} = \delta^{44/42}Ca_{hbl} - \delta^{44/42}Ca_{plg}$) of +0.12 ± 0.03 and +0.09 ± 0.04 respectively (Fig. 3). Clinopyroxenes (cpx) from eclogites and garnet peridotites have $\delta^{44/42}Ca$ ranging from +0.19 ± 0.02 to +0.35 ± 0.03, lower than their co-existing garnets (grt), which range from +0.33 ± 0.02 to +0.66 ± 0.03, with a $\Delta^{42/44}Ca_{grt-cpx}$ ($\Delta^{44/42}Ca_{grt-cpx} = \delta^{44/42}Ca_{grt} - \delta^{44/42}Ca_{cpx}$) ranging from +0.06 ± 0.03 to +0.38 ± 0.04 (Fig. 4a).

Despite their highly variable CaO contents, $\delta^{44/42}Ca$ of eight non-adakitic granitoids are similar, ranging from +0.33 ± 0.02 to +0.38 ± 0.02 with an average of +0.37 ± 0.03 (2SD, N = 8; Fig. 2). By contrast, nine low-Mg adakitic granitoids, with a narrow CaO range of 1.86–3.07 wt. %, have a significant $\delta^{44/42}Ca$ variation from +0.24 ± 0.02 to +0.38 ± 0.02, about five times larger than the analytical error. $\delta^{44/42}Ca$ of low-Mg adakitic granitoids are negatively correlated with $(Dy/Yb)_N$ (Fig. 5e). The $\varepsilon^{40/44}Ca$ of all granitoids studied here ranges from −0.1 to +1.4 with an average of +0.8 ± 0.9 (2SD, N = 17), slightly higher than the reported estimate values of bulk silicate Earth, which are −0.79 ± 0.60 (2SD, He et al., 2017a), −0.81 ± 0.61 (2SD, Simon et al., 2009) and −0.7 ± 0.5 (2SD, Mills et al., 2018), respectively.

5. DISCUSSION

5.1. Inter-mineral Ca isotope fractionation

5.1.1. Ca isotope fractionation between hornblende and plagioclase

Hornblende and plagioclase pairs from the Dabie granitoids most likely record equilibrium Ca isotope fractionation, because: first, no compositional zoning or heterogeneity has been identified in minerals (07LD-2 in Wu et al. (2017); 07YX-3 in Table S2); second, the coarse-grained granular texture implies that the studied granitoid minerals had enough time to equilibrate; and third, inter-mineral O and Fe isotopic equilibrium is achieved at crystallization temperature and is well preserved (Wu et al., 2017 and references therein).

Hornblende and plagioclase pairs from two Dabie granitoids have similar $\Delta^{44/42}Ca_{hbl-plg}$ (+0.12 ± 0.03 and +0.09 ± 0.04, respectively; Table 2). Inter-mineral Ca isotope fractionation factor is intrinsically controlled by the bonding environment of Ca^{2+}. Ca occupies the M4 site in hornblende, with a coordination number of 8 (Hawthorne and Oberti, 2007) and Ca—O bond length of 2.474 Å (tremolite, Zhou et al., 2016). The average coordination number of Ca in anorthite, the Ca end-member of plagioclase, is 6.75, with an average Ca—O bond length of 2.455 Å, slightly shorter than tremolite (Zhou et al., 2016). Because of their very close Ca—O bond lengths (i.e., average bonding energy of Ca—O bonds are similar), the total bonding energy of Ca^{2+} should be higher in a mineral with a larger coordination number (i.e., more Ca—O bonds). This may explain the heavier Ca isotopic composition of hornblende compared to plagioclase observed here. Based on the hornblende–plagioclase thermometry (Holland and Blundy, 1994), the equilibrium temperature of coexisting hornblende and plagioclase in 07LD-2 and 07YX-3 is estimated to be 663 °C and 761 °C respectively. Consequently, we estimate an equilibrium hornblende–plagioclase isotope fractionation factor,

$$\Delta^{44/42}Ca_{hbl-plg} = (+0.10 \pm 0.02) \times 10^6/T^2 \quad (3)$$

Table 1
Ca isotopic compositions of non-adakitic and low-Mg adakitic granitoids.

Samples	SiO_2 (wt.%)	MgO (wt.%)	CaO (wt.%)	$(Dy/Yb)_N$	$\delta^{44/40}Ca$	2SE	$\delta^{44/42}Ca$	2SE	$\varepsilon^{40/44}Ca$	2SE	n
Non-adakitic granitoids											
07FJS-2	57.41	5.84	6.96	1.25	0.72	0.04	0.36	0.02	0.42	0.28	7
Replicate					0.81	0.04	0.39	0.03	−0.14	0.54	8
Average					0.77	0.03	0.37	0.02	0.14	0.30	15
06TG-2	61.13	2.01	4.59	1.43	0.58	0.09	0.33	0.03	0.97	0.26	5
Replicate					0.65	0.02	0.34	0.04	0.48	0.76	8
Average					0.62	0.04	0.33	0.02	0.67	0.40	13
06ZY-2	66.95	1.65	3.11	1.04	0.74	0.03	0.38	0.02	0.51	0.22	8
07YC-1	72.70	0.58	1.60	1.75	0.62	0.05	0.37	0.02	1.43	0.38	8
07XM-1	68.18	1.14	2.55	1.32	0.64	0.02	0.37	0.02	1.37	0.52	8
06TG-1	62.24	1.54	4.57	1.60	0.68	0.05	0.36	0.03	0.53	0.41	6
07YC-3	70.60	0.47	1.59	1.59	0.61	0.03	0.36	0.02	1.36	0.38	6
07YX-2	59.74	2.51	5.15	-	0.78	0.05	0.38	0.02	−0.08	0.49	6
Low-Mg adakitic granitoids											
07FJ-2	69.56	0.81	2.10	1.91	0.56	0.02	0.32	0.01	1.11	0.30	8
07FJ-6	68.70	1.46	3.07	1.27	0.68	0.02	0.38	0.02	1.16	0.42	8
07LS-5	70.83	0.62	2.33	3.12	0.39	0.03	0.23	0.02	0.86	0.54	8
Replicate					0.49	0.04	0.26	0.03	0.38	0.52	8
Average					0.44	0.02	0.24	0.02	0.62	0.37	16
07ZB-1	68.67	0.91	2.14	3.00	0.47	0.04	0.28	0.03	1.10	0.47	8
07ZB-6	65.75	1.29	2.71	2.67	0.51	0.03	0.29	0.02	1.01	0.30	8
07LD-2	68.65	1.32	2.50	1.46	0.63	0.04	0.34	0.03	0.72	0.46	8
EGB-2	69.94	0.64	1.86	1.54	0.64	0.02	0.35	0.02	0.90	0.31	8
YFD-3	69.55	0.88	2.17	2.51	0.50	0.08	0.25	0.03	1.09	2.16	5
Replicate					0.49	0.04	0.28	0.03	0.72	0.77	8
Triplicate					0.58	0.05	0.30	0.02	0.44	0.26	8
Average					0.53	0.03	0.28	0.02	0.48	0.77	21
YFD-8	68.72	1.24	2.42	2.16	0.47	0.06	0.24	0.04	0.46	0.52	8
Replicate					0.58	0.04	0.27	0.05	−0.36	0.71	7
Triplicate					0.55	0.04	0.28	0.01	0.32	0.41	8
Average					0.53	0.03	0.26	0.02	0.16	0.32	23
Standards											
SRM 915b					0.75	0.02	0.35	0.01	−0.29	0.20	73
Lit. value[a]					0.79	0.02	0.36	0.01	−0.60	0.16	41
IAPSO seawater					1.87	0.02	0.90	0.01	−0.27	0.17	66
Lit. value[a]					1.89	0.02	0.91	0.01	−0.31	0.16	147
Lit. value[b]					1.86	0.05					
BCR-2					0.83	0.04	0.40	0.02	−0.23	0.34	15
Lit. value[a]					0.80	0.02	0.38	0.01	−0.17	0.28	30
Lit. value[c]					0.79	0.02					24
BHVO-1					0.77	0.04	0.36	0.02	−0.35	0.45	7
Lit. value[c]					0.77	0.06					3
BHVO-2					0.84	0.02	0.39	0.02	−0.44	0.28	11
Lit. value[a]					0.79	0.01	0.38	0.01	−0.24	0.17	58
Lit. value[c]					0.77	0.03					12

Notes: The δ values are referenced to NIST SRM 915a.
References:
[a] He et al. (2017a).
[b] Amini et al. (2009).
[c] Feng et al. (2017).

which is consistent with that obtained by first-principles calculations (Fig. 3; Zhou et al., 2016). Uncertainties in the equations for fractionation factors are given as two standard errors of the mean in this study if not specified.

Combined with the estimated clinopyroxene–melt and plagioclase–melt Ca isotope fractionation factors in Zhang et al. (2018), Ca isotope fractionation factors between Ca bearing minerals and melt are:

$$\Delta^{44/42}Ca_{plg-melt} = (-0.07 \pm 0.04) \times 10^6/T^2 \quad (4)$$

$$\Delta^{44/42}Ca_{hbl-melt} = (+0.03 \pm 0.05) \times 10^6/T^2 \quad (5)$$

$$\Delta^{44/42}Ca_{cpx-melt} = (+0.04 \pm 0.03) \times 10^6/T^2 \quad (6)$$

respectively.

Table 2
Ca isotope compositions of mineral pairs.

	Hornblende			Plagioclase				
	$\delta^{44/42}$Ca	2SE	n	$\delta^{44/42}$Ca	2SE	n	$\Delta_{hbl-plg}$	2SE
Dabie granitoids								
07LD-2	0.43	0.02	7	0.32	0.02	7	0.12	0.03
07YX-3	0.44	0.03	7	0.35	0.03	7	0.09	0.04
	Garnet			Clinopyroxene				
	$\delta^{44/42}$Ca	2SE	n	$\delta^{44/42}$Ca	2SE	n	$\Delta_{grt-cpx}$	2SE
Dabie eclogites								
BXL-1	0.36	0.03	10	0.27	0.03	6		
Replicate	0.30	0.03	8					
Average	0.33	0.02	18				0.06	0.03
BXL-4	0.60	0.03	10	0.30	0.01	10		
Replicate	0.58	0.03	8	0.27	0.03	8		
Average	0.59	0.02	18	0.29	0.02	18	0.31	0.02
BXL-6	0.66	0.03	8	0.28	0.03	8	0.38	0.04
HA-3	0.61	0.04	8	0.26	0.03	8		
Replicate	0.61	0.04	8	0.22	0.03	8		
Average	0.61	0.03	16	0.24	0.02	16	0.38	0.04
HA-4	0.57	0.04	8	0.18	0.03	8		
Replicate	0.55	0.05	8	0.19	0.03	8		
Average	0.56	0.03	16	0.19	0.02	16	0.37	0.04
SH-1	0.57	0.02	8	0.33	0.03	8	0.24	0.04
SH-5	0.58	0.02	8	0.35	0.03	8	0.23	0.04
Sulu garnet peridotites								
ZMF-2	0.64	0.03	8	0.34	0.02	8	0.31	0.04
ZMF-3	0.64	0.05	8	0.34	0.02	8	0.30	0.05

Notes: The δ values are referenced to NIST SRM 915a. $\delta^{44/40}$Ca and $\varepsilon^{40/44}$Ca values are listed in Table S1.

5.1.2. Ca isotope fractionation between garnet and clinopyroxene

The garnet–clinopyroxene equilibrium temperatures are calculated using the Fe–Mg exchange thermometer (Li et al., 2011; Li et al., 2016; Table S3). $\Delta^{42/44}Ca_{grt-cpx}$ do not plot on a single temperature-dependent trend (Fig. 4a), indicating either isotopic disequilibrium or a possible mineral compositional control on $\Delta^{42/44}Ca_{grt-cpx}$ (e.g., Feng et al., 2014; Wang et al., 2017a,b). The mineral composition homogeneity of garnet and clinopyroxene in Dabie eclogites measured here has been previously checked by electron microprobe analyses on multiple grains (Li et al., 2011; Li et al., 2016) and is indexed by relative standard derivation (RSD in %) of CaO of minerals in individual samples. As shown in Fig. S2, RSD (%) of CaO for garnet and clinopyroxene in individual samples ranges from <1% to 22%, indicating significant chemical heterogeneity in some samples, especially in HA-3 and HA-4 that have the lowest peak metamorphic temperature (Fig. S2; Li et al., 2016). In contrast, duplicate measurements on mineral separates of BXL-1, BXL-4, HA-3 and HA-4, which were measured on independent dissolution of different splits (typically ~20 grains each), have the same $\delta^{44/42}$Ca values (Fig. S2; Table 2), suggesting homogeneous Ca isotopic compositions of the individual minerals on a grain scale. In addition, except for BXL-1, mineral pairs from the Dabie eclogites define a single trend on the plot of $\Delta^{44/42}$Ca vs. $1/T^2$ (Fig. 4a), irrespective of RSD (%) of CaO for garnet and clinopyroxene (Fig. S2). We thus suggest that Ca isotope equilibrium most likely has been reached during metamorphic recrystallization and well preserved since the peak metamorphism (Li et al., 2016). This inference is supported by available Mg isotopic data on the same set of samples. RSD (%) of MgO content for garnet and clinopyroxene in Dabie elogites ranges from 1% to 36%, but Mg isotope equilibrium has been documented between these two minerals (Li et al., 2011; Li et al., 2016), indicating post crystallization diffusion could be insignificant despite the presence of chemical gradient. Given the much slower diffusion rate of Ca than Mg (Perchuk et al., 2009; Zhang et al., 2010), post crystallization diffusive exchange of Ca between garnet and clinopyroxene should be also insignificant, which thus supports the preservation of isotope equilibrium during metamorphic recrystallization. The coarse-grained granular texture (Liu et al., 2015) and homogeneous mineral compositions in the eclogite BXL-1 and Zhimafang garnet peridotites (Li et al., 2011; Fig. S3; Table S3) support that Ca isotope equilibrium has been reached between garnet and clinopyroxene.

In clinopyroxene ($^{M2}X^{M1}YSi_2O_6$), large cations such as Ca^{2+} and Na^{+} preferentially occupy the eight-fold coordinated M2 site while smaller cations (e.g., Mg^{2+}, Fe^{2+}, Fe^{3+} and Al^{3+}) prefer the six-fold coordinated M1 site. Our studied clinopyroxenes have Ca/(Ca + Mg + Fe) of 0.43–0.48, so that Ca^{2+} occupies only the eight-fold coordinated sites (Li et al., 2011; Li et al., 2016; Table S3), with a Ca—O bond length of 2.45–2.50 Å (Shannon, 1976; Smyth

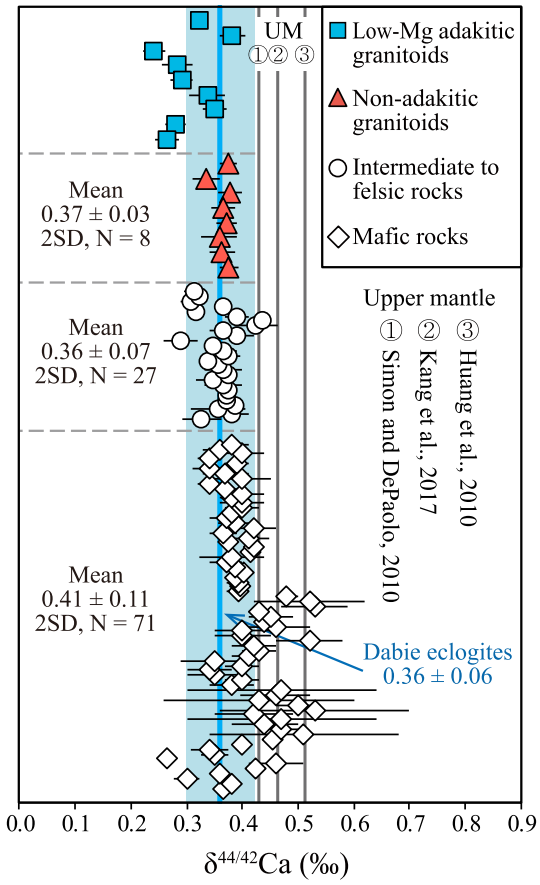

Fig. 2. Ca isotopic compositions of Dabie low-Mg adakitic and non-adakitic granitoids. Data for terrestrial mafic to felsic rocks are from Amini et al. (2009); Huang et al. (2010); Simon and DePaolo (2010); Huang et al. (2011); Valdes et al. (2014); Jacobson et al. (2015); Feng et al. (2017); He et al. (2017a); Liu et al. (2017a, b); Zhang et al. (2018); Zhu et al. (2018). The error bars represent 2SE uncertainties. The estimate of upper mantle from Huang et al. (2010); Simon and DePaolo (2010) and Kang et al. (2017) are also shown. The blue vertical band represents the Dabie eclogites compositions of +0.36 ± 0.06 (2SD, Lu et al., 2017). The $\delta^{44/42}$Ca of reference data is calculated by $\delta^{44/42}Ca = \delta^{44/40}Ca/2.0483$ (Farkaš et al., 2011; Huang et al., 2012) if there is only $\delta^{44/40}$Ca reported. Note that errors may arise due to nonzero $\varepsilon^{40/44}$Ca, which, however, could be minor for basaltic samples, e.g., <0.04 on $\delta^{44/42}$Ca (He et al., 2017a).

and Bish, 1988; Feng et al., 2014; Wang et al., 2017b). In garnet ($^{M2}X_3\ ^{M1}Y_2(SiO_4)_3$), Ca preferentially occupies the eight-fold coordinated M2 site with a Ca—O bond length ranging from 2.27 to 2.43 Å (Novak and Gibbs, 1971; Huang et al., 2019). The difference in Ca—O bonds between garnet and clinopyroxene explain why garnet has heavier Ca isotopic composition than its co-existing clinopyroxene (Magna et al., 2015; Huang et al., 2019), which is opposite to what is observed for Mg isotopes. Garnet shows a Mg isotopic composition much lighter than clinopyroxene (e.g., Li et al., 2011; Li et al., 2016).

Garnet–clinopyroxene pairs from eclogites and garnet peridotites form three groups in a plot of $\Delta^{44/42}Ca_{grt-cpx}$ vs. $1/T^2$ (Fig. 4a). Most pairs plot on a positive trend with $\Delta^{44/42}Ca_{grt-cpx} = +0.21 \times 10^6/T^2$. BXL-1 eclogite plots

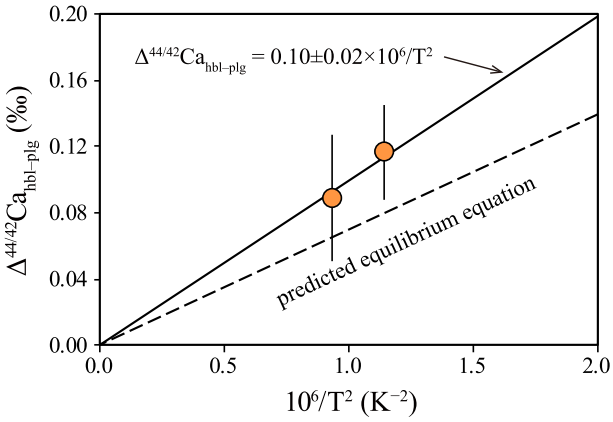

Fig. 3. Ca isotope fractionation between coexisting hornblende and plagioclase. The solid line represents the equilibrium equation calibrated with hornblende and plagioclase pairs in this study ($\Delta^{44/42}Ca_{hbl-plg} = 0.10 \pm 0.02 \times 10^6/T^2$). The calculated equilibrium temperature according to hornblende–plagioclase thermometry is 663 °C and 761 °C (Holland and Blundy, 1994; Table S2). The predicted equilibrium equation using first-principles calculations is shown as the dash line (Zhou et al., 2016). The error bars represent 2SE uncertainties.

below this trend with a lower $\Delta^{44/42}Ca_{grt-cpx}$, and Zhimafang garnet peridotites plot above this trend with higher $\Delta^{44/42}Ca_{grt-cpx}$. If the observed inter-mineral Ca isotopic difference reflects equilibrium isotope fractionation, those variable $\Delta^{44/42}Ca_{grt-cpx}$ at a given temperature must reflect a mineral composition effect on inter-mineral isotope fractionation. To evaluate the potential mineral compositional control, $A_{grt-cpx} = \Delta^{44/42}Ca_{grt-cpx} \times T^2/10^6$, representative of isotope fractionation with the temperature effect corrected, is plotted against mineral compositions. Studied garnets have highly variable compositions with Ca/(Mg + Fe + Ca) ranging from 0.12 to 0.30 (Fig. 4b). The predicted $A_{grossular-diopside}$ by first-principles calculations ($A_{grossular-diopside}$ = +0.28, Huang et al., 2019) is higher than mineral pairs from Dabie eclogite while lower than that from Sulu garnet peridotite with the largest Ca content in garnet. And BXL-1 in Dabie mineral samples, with garnet Ca/(Ca + Mg + Fe) of 0.21, yields a very low $A_{grt-cpx}$. Ca—O bond length in orthopyroxene decreases significantly when Ca/(Ca + Mg) is lower than 1/8 (Wang et al., 2017b). Although the variation of Ca—O bond length in garnet at low Ca content is not clear now, this effect should be very limited due to the fact that Ca content of our garnet samples are high enough (>1/8) (Fig. 4b). Therefore, we suggest that the Ca isotope fractionation between garnet and clinopyroxene is not controlled by the composition of garnet. This is further supported by whole rock data of low-Mg adakitic granitoids (Section 5.2.2).

The equilibrium isotope fractionation between two phases can be expressed using β-factors, which measures the equilibrium isotope fractionation between the phase of interest and an atomic gas, as: $\Delta_{A-B} = 10^3 \ln\alpha_{A-B} = 10^3 \ln\beta_A - 10^3 \ln\beta_B$ (Richet et al., 1977). Wang et al. (2017b) investigated the Ca concentration effect on the $10^3 \ln\beta^{44/40Ca}$ of clinopyroxene with a chemical formula of $Ca_xMg_{1-x}SiO_3$ using first-principles calculations. Diopside

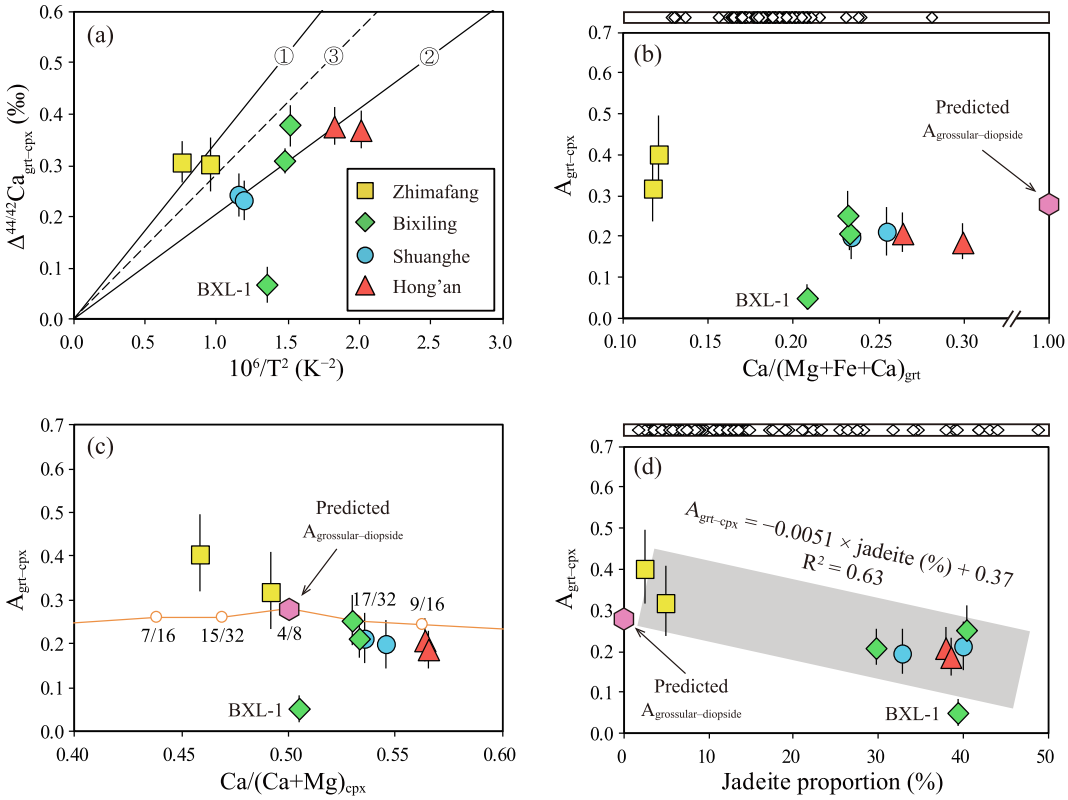

Fig. 4. (a) Ca isotope fractionation between coexisting garnet and clinopyroxene. The error bars represent 2SE uncertainties. Equilibrium temperatures are from Li et al. (2011); Li et al. (2016) and Table S3. The lines 1 and 2 represent linear fits with intercept = 0 for mineral pairs from Shuanghe, Hong'an and Bixiling eclogites ($\Delta^{44/42}Ca_{grt-cpx} = +0.21 \times 10^6/T^2$; BXL-1 as an outlier) and those for two Zhimafang garnet peridotites ($\Delta^{44/42}Ca_{grt-cpx} = +0.35 \times 10^6/T^2$) respectively. The predicted Ca isotope fractionation between grossular and diopside using first-principles calculations is shown as the dash line 3 (Huang et al., 2019). (b) $A_{grt-cpx}$ vs. Ca/(Mg + Fe + Ca) (in a mole ratio) in garnet. $A = \Delta^{44/42}Ca \times T^2/10^6$. Predicted $A_{grosslar-diopside}$ is according to Huang et al. (2019). (c) $A_{grt-cpx}$ vs. Ca/(Ca + Mg) (in a mole ratio) of clinopyroxene. Orange line represents the predicted variation of $A_{grt-cpx}$ with different Ca/(Ca + Mg) of clinopyroxene according to Wang et al. (2017b). (d) $A_{grt-cpx}$ vs. jadeite proportion (%) in clinopyroxene. Jadeite proportion (%) in clinopyroxene is calculated following Morimoto (1988). Open diamonds in bars above (b) and (d) show Ca/(Mg + Fe + Ca) of garnet and jadeite proportion (%) in clinopyroxene in the residua from partial melting experiments of basaltic materials at 0.8–3.8 GPa, respectively (Sen and Dunn, 1994; Rapp, 1995; Rapp and Watson, 1995; Winther, 1996; Rapp et al., 1999; Xiong et al., 2005). The error bars in (b), (c) and (d) are calculated according to 2SE uncertainties of $\Delta^{44/42}Ca_{grt-cpx}$ and T.

($MgCaSi_2O_6$), with a Ca/(Ca + Mg) of 1/2, has the longest Ca—O bond length and accordingly the lowest $10^3 ln\beta^{44/40Ca}$. $10^3 ln\beta^{44/40Ca}$ of clinopyroxene increases with increasing Ca content when Ca/(Ca + Mg) < 1/2, and decreases with increasing Ca content when Ca/(Ca + Mg) > 1/2 (Wang et al., 2017b). Nevertheless, the effect of Ca/(Ca + Mg) on $10^3 ln\beta^{44/40Ca}$ of clinopyroxene is small, on the order of 0.06 compared to 0.35 in observed $A_{grt-cpx}$, and cannot account for the variation in Ca isotope fractionation between garnet and clinopyroxene in this study (Fig. 4c). As shown in Fig. 4d, Zhimafang samples with high $A_{grt-cpx}$ have low jadeite proportion in clinopyroxene (~4%, calculated following Morimoto (1988)), while other samples with low $A_{grt-cpx}$ have relatively high jadeite proportion (30–40%). Notably, the average bond length between cation in the M2 site and oxygen in clinopyroxene ($XYSi_2O_6$) changes by ~0.01 Å when jadeite proportion increase from 0 to 53% at a given pressure (Nestola et al., 2008). Na^+ is similar in size to Ca^{2+} but has a lower electronegativity than Ca^{2+} (Allred, 1961), and bond length has a negative correlation with electronegativity (Dimitrov and Komatsu, 2012). Therefore, we speculate that the Ca—O bond length may decrease with increasing $Na^+ + Al^{3+}$ component (i.e., jadeite component) in clinopyroxene due to the longer Na—O bonds. This calls on future confirmation by theoretical calculation and/or experimental calibration. In this study, we attribute the fractionation caused by jadeite component in clinopyroxene to the jadeite effect.

Consequently, we suggest that the variation in $A_{grt-cpx}$ is controlled by the jadeite effect (Fig. 4d). A linear regression between $A_{grt-cpx}$ and jadeite component proportion in clinopyroxene is fitted with $A_{grt-cpx} = (-0.0051 \pm 0.0029) \times jadeite(\%) + (0.37 \pm 0.10)$ (2SE, 95% c.i.; $R^2 = 0.63$). Given insignificant Ca isotope fractionation during crystallization of clinopyroxene with very low Na content (<<1%) observed in the Kilauea Iki lava lake at Hawaii (Zhang et al., 2018), the fractionation factor between the melt

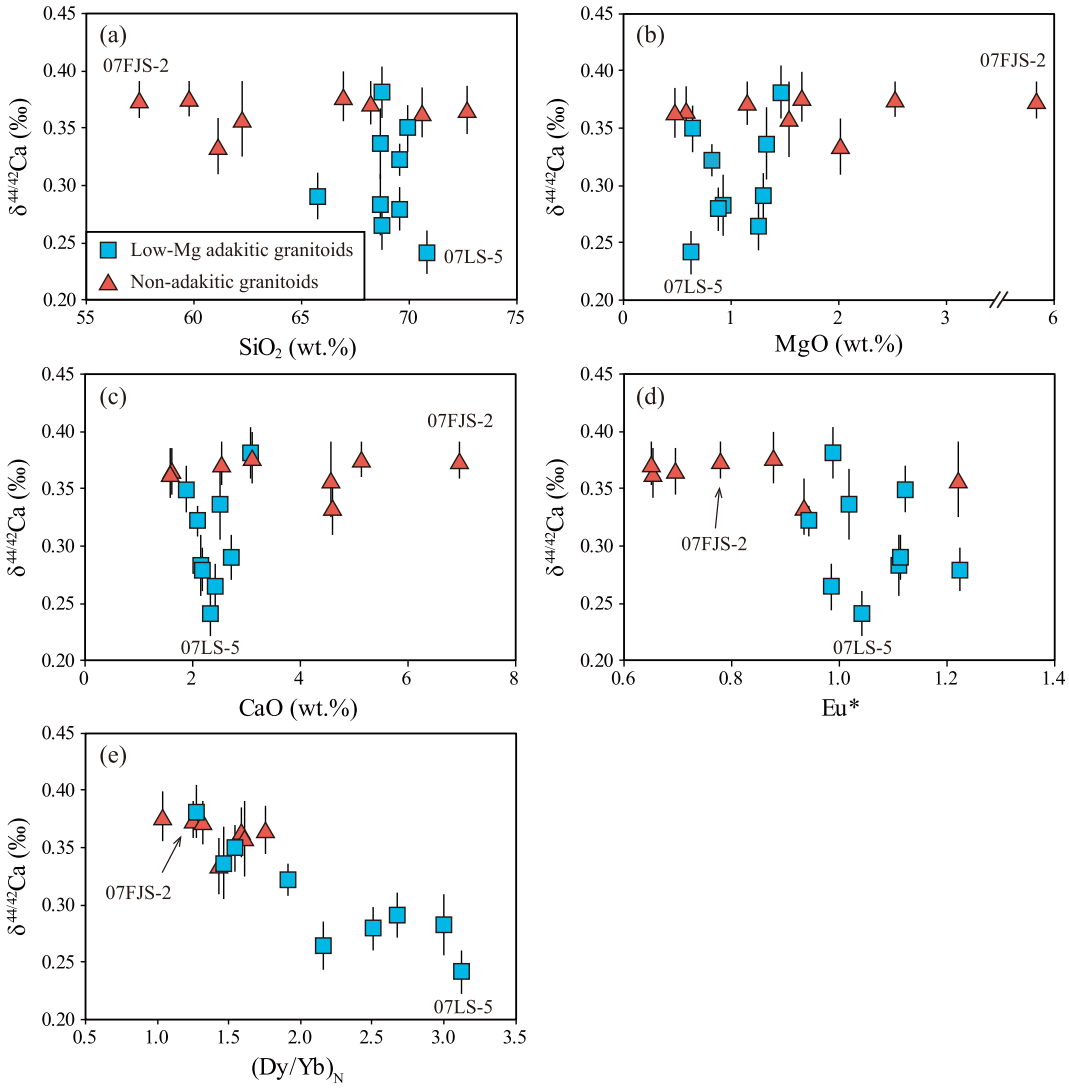

Fig. 5. $\delta^{44/42}$Ca vs. SiO_2 (a), MgO (b), CaO (c), Eu^* (d) and $(Dy/Yb)_N$ (e) for Dabie granitoids. $Eu^* = Eu_N/(Sm_N \times Gd_N)^{1/2}$. Subscript N represents normalization to the chondrite values (Sun and McDonough, 1989). Major and trace element data are from Wang et al. (2007) and He et al. (2011).

and clinopyroxene with no jadeite component is estimated to be 0 at magmatic temperature. Therefore, $\Delta^{44/42}Ca_{cpx-melt}$ and $\Delta^{44/42}Ca_{grt-melt}$ are given:

$$\Delta^{44/42}Ca_{cpx-melt} = (+0.0051 \pm 0.0029) \times jadeite(\%) \times 10^6/T^2 \quad (7)$$

$$\Delta^{44/42}Ca_{grt-melt} = (+0.37 \pm 0.10) \times 10^6/T^2 \quad (8)$$

which is consistent with the equilibrium Ca isotope fractionation between grossular and diopside (clinopyroxene with no jadeite component) predicted by first-principles calculations ($\Delta^{44/42}Ca_{grt-cpx} = +0.28 \times 10^6/T^2$, Huang et al., 2019).

5.2. Ca isotope variation of Dabie granitoids

Calcium isotopic compositions of Dabie granitoids could be potentially affected by weathering, magma differentiation, partial melting and source heterogeneity. All studied samples, except for 07FJS-2 and 07LS-5, are not altered (Fig. S1). They have loss on ignition (LOI) below 2.2 wt.% and chemical index of alteration (CIA) of 47.1–50.8, (Fig. 6), arguing against a significant role of weathering. Samples 07FJS-2 and 07LS-5 have relatively high LOI (2.35 wt.% and 3.75 wt.%), and kaolinization of plagioclase has been observed. They are thus labeled in all figures. $\delta^{44/42}$Ca of 07FJS-2 ($+0.36 \pm 0.02$) is similar to other non-adaktic granitoids ranging from $+0.33 \pm 0.02$ to $+0.38 \pm 0.02$ (Fig. 5 and Table 1). Despite its lowest $\delta^{44/42}$Ca ($+0.24 \pm 0.02$), sample 07LS-5 falls on the compositional trends defined by the other low-Mg adaktic granitoids (Fig. 5). Therefore, weathering does not significantly affect $\delta^{44/42}$Ca of these two samples at the scale of our analytical uncertainty (±0.03). In the following, we focus on the evaluation of Ca isotope fractionation during crustal melting and magma differentiation.

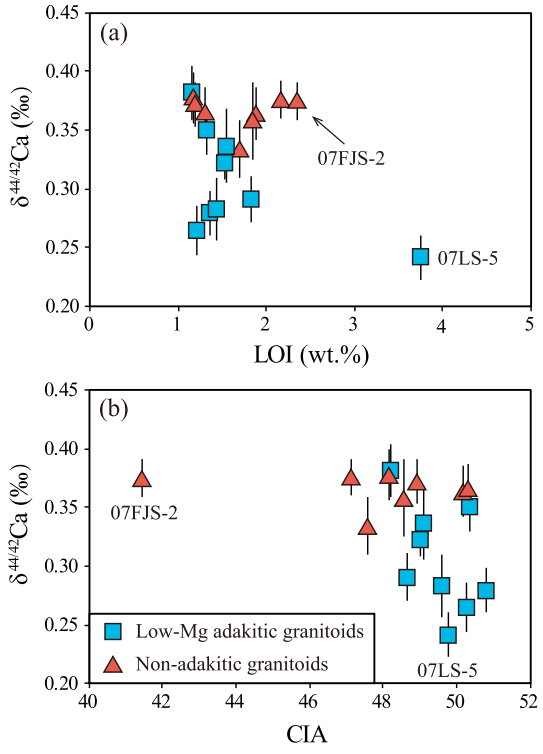

Fig. 6. $\delta^{44/42}$Ca vs. LOI (a) and CIA (b) for Dabie granitoids. LOI and CIA data are from Wang et al. (2007) and He et al. (2011). CIA (chemical index of alteration) = $n(Al_2O_3)/[n(Al_2O_3) + n(CaO^*) + n(Na_2O) + n(K_2O)] \times 100$, where CaO^* is the amount of CaO incorporated in the silicate fraction of the rock (Nesbitt and Young, 1982).

5.2.1. Homogeneous Ca isotopic compositions of Dabie non-adakitic granitoids

Dabie non-adakitic granitoids have highly variable compositions, which can be partially attributed to fractional crystallization of clinopyroxene, hornblende, plagioclase and K-feldspar (e.g., Wang et al., 2007; He et al., 2011; He et al., 2017b). However, they have homogeneous Ca isotopic compositions, with a mean $\delta^{44/42}$Ca value of +0.37 ± 0.03 (2SD, N = 8) (Fig. 5), indicating that Ca isotope fractionation is insignificant during fractionation of a mineral assemblage involving clinopyroxene with nearly no jadeite component (Ma et al., 1998), hornblende, plagioclase, ± other Ca depleted minerals. This inference is consistent with the available mineral–melt Ca isotope fractionation factors. Specifically, $\Delta^{44/42}Ca_{plg-melt}$, $\Delta^{44/42}Ca_{hbl-melt}$ and $\Delta^{44/42}Ca_{cpx-melt}$ (clinopyroxene here has nearly no jadeite component) are estimated at −0.05 ± 0.03, +0.02 ± 0.03 and +0.03 ± 0.02 at 900 °C, respectively, according to Eqs. (4), (5) and (6) in Section 5.1.1.

Given the low $(Dy/Yb)_N$ of non-adakitic granitoids (Fig. S4), garnet may not play an important role in their petrogenesis, while clinopyroxene, hornblende and plagioclase are likely prevailing in their residua (Wang et al., 2007; He et al., 2011 and references therein). Based on the discussion above, Ca isotope fractionation between melts and those residual minerals (low jadeite clinopyroxene, hornblende and plagioclase) is limited (this study; Zhang et al., 2018). Non-adakitic granitoids have $\delta^{44/42}$Ca of +0.37 ± 0.03 (2SD, N = 8) which is similar to the local basement (+0.36 ± 0.06, 2SD, Lu et al., 2017). Therefore, we infer insignificant Ca isotope fractionation during low pressure crustal melting without residual garnet (depth < ca. 40 km) which produced those non-adakitic granitoids (He et al., 2011).

5.2.2. Significant Ca isotope fractionation in Dabie low-Mg adakitic granitoids due to residual garnet and jadeite-rich clinopyroxene

In contrast to non-adakitic granitoids, low-Mg adakitic samples have significantly variable $\delta^{44/42}$Ca ranging from +0.24 ± 0.02 to +0.38 ± 0.02. This observed $\delta^{44/42}$Ca variation cannot be explained by fractional crystallization, given the narrow SiO_2, MgO, CaO and Eu^* ranges of the low-Mg adakitic samples that argues against substantial fractional crystallization (Fig. 5a–d). Moreover, the mineral assemblage of low-Mg adakitic granitoids is similar to that of non-adakitic granitoids with similar major element compositions (Wang et al., 2007; He et al., 2011). The limited Ca isotope fractionation among non-adaktic granitoids indicates that fractional crystallization of such a mineral assemblage, if any, cannot significantly affect the melt $\delta^{44/42}$Ca (Section 5.2.1). Their $^{87}Sr/^{86}Sr(i)$ and $\varepsilon_{Nd}(t)$ are variable, with $^{87}Sr/^{86}Sr(i)$ ranging from 0.70699 to 0.70864 and $\varepsilon_{Nd}(t)$ ranging from −15.57 to −24.25. $\delta^{44/42}$Ca is not correlated with $^{87}Sr/^{86}Sr(i)$ or $\varepsilon_{Nd}(t)$ (Fig. 7), indicating that source $\delta^{44/42}$Ca heterogeneity does not account for the Ca isotopic variation observed in low-Mg adakitic granitoids.

$\delta^{44/42}$Ca of low-Mg adakitic granitoids negatively correlate with $(Dy/Yb)_N$ (Fig. 5e), which suggests residual garnet plays a role in Ca isotope variation (He et al., 2017a). The highly variable $(Dy/Yb)_N$ suggests that low-Mg adakitic granitoids are derived from a series of thickened mafic LCC leaving residua of variable garnet and clinopyroxene proportions, e.g., from 5% garnet +95% clinopyroxene to 30% garnet +70% clinopyroxene (He et al., 2011). To quantitatively constrain the isotopic effect of residual mineral assemblage, Ca isotope fractionation during crustal melting is modelled using equations modified after He et al. (2017b), assuming $\delta^{44/42}Ca_{residue} \approx \delta^{44/42}Ca_{source}$ due to the low CaO content of low-Mg adakitic granitoids compared to the basaltic sources and low degree of partial melting (~5%):

$$\delta^{44/42}Ca_{melt} \approx \delta^{44/42}Ca_{source} + \Delta^{44/42}Ca_{melt-residue} \quad (9)$$

where

$$\Delta^{44/42}Ca_{melt-residue} = f_{grt} \times \Delta^{44/42}Ca_{melt-grt} + (1 - f_{grt}) \times \Delta^{44/42}Ca_{melt-cpx}$$

f_{grt} ($f_{grt} = \frac{D(CaO)_{grt/cpx} \times R_{grt}}{R_{cpx} + D(CaO)_{grt/cpx} \times R_{grt}}$) represents the Ca fraction of garnet in the residue. $D(CaO)_{grt/cpx}$ represents the partitioning coefficient of CaO between garnet and clinopyroxene. R represents the mineral proportion in the residue. Combined Eq. (9) and Eqs. (7) and (8) in Section 5.1.2, then,

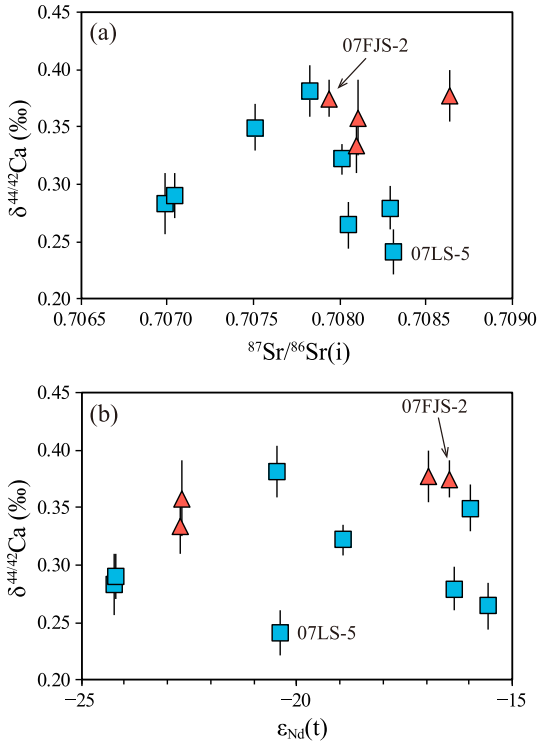

Fig. 7. $\delta^{44/42}$Ca vs. $^{87}Sr/^{86}Sr$(i) (a) and ε_{Nd}(t) (b) for Dabie low-Mg adakitic granitoids. Sr–Nd isotopic compositions are from Wang et al. (2007) and He et al. (2013).

$$\delta^{44/42}Ca_{melt} = \delta^{44/42}Ca_{melt} - f_{grt} \times 0.37 \times \frac{10^6}{T^2} - (1 - f_{grt}) \times 0.0051 \times jadeite(\%) \times 10^6/T^2 \quad (10)$$

where $\delta^{44/42}Ca_{source}$ is assumed to be the mean value of local eclogites (+0.36 ± 0.06, 2SD, Lu et al., 2017). Initial magma temperature of Dabie low-Mg adakitic granitoids could be >1075 °C (Xiao and Clemens, 2007) and 1100 °C is adopted here. $D(CaO)_{grt/cpx}$ is estimated according to its good correlation with jadeite proportion in clinopyroxene (Fig. S5; Rapp and Watson, 1995), and R_{grt} is constrained by $(Dy/Yb)_N$ after He et al. (2011).

To evaluate whether the role of residual garnet is sufficient to explain the data of low-Mg adakitic granitoids, a simple model is considered here without taking into account the effect of jadeite component in clinopyroxene (Section 5.1.2). By setting jadeite (%) in the Eq. (10) to 0, the calculated fractionation during eclogite melting can only account for 1/3 of the $\delta^{44/42}$Ca variation observed in low-Mg adakitic granitoids at a given $(Dy/Yb)_N$ (Fig. 8; Table 3). In the following, we will discuss the jadeite effect on the $\delta^{44/42}$Ca variation of low-Mg adakitic granitoids.

High pressure experiments show that the jadeite proportion in clinopyroxene increases with increasing pressure (Fig. S6; Sen and Dunn, 1994; Rapp, 1995; Rapp and Watson, 1995; Winther, 1996; Rapp et al., 1999; Xiong et al., 2005). Applying Eq. (10) and He et al. (2011)'s model for trace elements to the 3.2 GPa runs in Rapp and Watson (1995), the predicted melt has $\delta^{44/42}$Ca as low as +0.22 and $(Dy/Yb)_N$ of 3.75 (Table 3). Binary mixing could explain

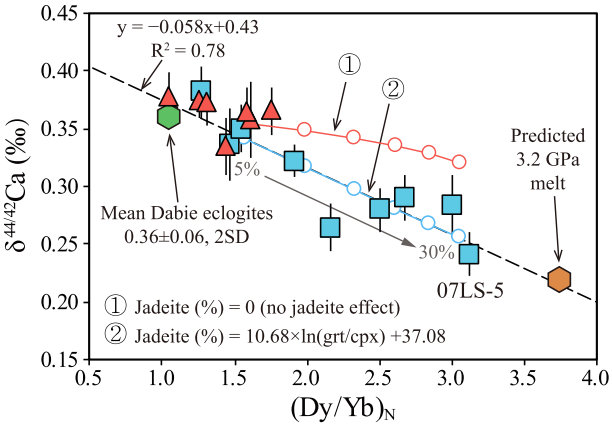

Fig. 8. Comparison of the model calculation results with observed Dabie low-Mg adakitic granitoids in the $\delta^{44/42}$Ca vs. $(Dy/Yb)_N$ diagram. The black dash line represents a linear regression of Dabie low-Mg adakitic granitoids. Curve 1 represents the largest predicted garnet effect during partial melting, given that $D(CaO)_{grt/cpx}$ is assumed to the largest estimated value (0.60) observed in Rapp and Watson (1995) (Fig. S5); Curve 2 represents predicted partial melts taking the isotopic effect of both the residual garnet and jadeite-rich clinopyroxene into account and assuming a relationship between jadeite proportion (%) in clinopyroxene and grt/cpx (jadeite (%) = 10.68 × ln(grt/cpx) + 37.08). Parameters used in the calculations of Curve 1 and 2 are listed in Table 3. Segments on curves remark 5% increments in residual garnet fraction. The mean composition of Dabie basement eclogites (Lu et al., 2017) and a predicted 3.2 GPa melt based on fractionation factors in this study and experimental data from Rapp and Watson (1995) are also plotted for a comparison.

the negative correlation between $\delta^{44/42}$Ca and $(Dy/Yb)_N$ of low-Mg adakitic granitoids, e.g., between one end-member with low $\delta^{44/42}$Ca and high $(Dy/Yb)_N$ from high pressure melting and the other end-member with unfractionated $\delta^{44/42}$Ca and $(Dy/Yb)_N$ from shallow depths (e.g., Dabie non-adakitic granitoids). The absence of a correlation between $\delta^{44/42}$Ca and CaO requires that those two end-member should have similar CaO contents. Non-adakitic granitoids, however, have higher Yb/CaO than those of low-Mg adakitic ones at a given CaO (Fig. S7). Mixing between either the predicted 3.2 GPa melt or the low-Mg adakitic sample 07LS-5 with the lowest $\delta^{44/42}$Ca in our study and a non-adakitic end-member cannot explain the linear trend of low-Mg adakitic granitoids in the diagrams of $\delta^{44/42}$Ca vs. $(Dy/Yb)_N$ and Yb/CaO (Figs. 8 and S7).

Given the high and correlated Sr/Y, $(La/Yb)_N$, $(Dy/Yb)_N$ and Nb/Ta of Dabie adakitic granitoids, Dabie low-Mg adakitic granitoids may derive from low degree partial melting (~5%) of sources with various proportions of residual clinopyroxene and garnet (He et al., 2011). The correlation between $\delta^{44/42}$Ca and $(Dy/Yb)_N$ for low-Mg adakitic granitoids most likely reflects differences in mineralogy in their sources. Since $(Dy/Yb)_N$ of melt is dominantly governed by the garnet abundance in the residua (He et al., 2011), the observed trend requires an isotopic effect of jadeite-rich clinopyroxene varied with the residual

Table 3
Parameters adopted and modelling results for partial melting.

	Source composition	Partition coefficient	
		Garnet	Clinopyroxene
Dy	3.1	4.4	1.2
Yb	1.5	14	0.9
$\delta^{44/42}$Ca	0.36 ± 0.06		
Calculated melts for 5% degree of eclogitic partial melting at 1100 °C			
Source mineralogy	$(Dy/Yb)_N$	$\delta^{44/42}$Ca	
		1[a]	2[a]
5% grt + 95% cpx	1.57	0.35	0.34
10% grt + 90% cpx	1.99	0.35	0.32
15% grt + 85% cpx	2.33	0.34	0.30
20% grt + 80% cpx	2.61	0.33	0.28
25% grt + 75% cpx	2.85	0.33	0.27
30% grt + 70% cpx	3.05	0.32	0.25
Predicted 3.2 GPa melt			
55% grt + 45% cpx	3.75	0.28	0.22

Notes: Dy and Yb contents of source are approximated to the mean lower continental crust (Rudnick and Gao, 2003). Partial melting temperature is assumed to be 1100 °C according to Xiao and Clemens (2007). $\delta^{44/42}$Ca of source are approximated to that of Dabie eclogites (Lu et al., 2017). Partition coefficients for garnet and clinopyroxene are from the compilation of He et al. (2011). $(Dy/Yb)_N$ of melts are calculated according to the batch melting model modified after He et al. (2011). $\delta^{44/42}$Ca of melts are calculated using Eq. (10) in the main text. The superscript a denotes: 1, predicted melts considering the garnet effect only, given that $D(CaO)_{grt/cpx}$ is assumed to the largest estimated value (0.60) observed in Rapp and Watson (1995) (Fig. S5); 2, predicted melts considering the isotopic effect of both residual garnet and jadeite-rich clinopyroxene, assuming a relationship between jadeite (%) in clinopyroxene and grt/cpx (jadeite (%) = 10.68 × ln(grt/cpx) + 37.08).

garnet abundance (e.g., jadeite (%) = 10.68 × ln(grt/cpx) + 37.08; Fig. 8). Note that the relationship between jadeite (%) and grt/cpx depends on the regression of the compositional isotope effect of clinopyroxene in Fig. 4c, which calls on future calibration. The lowest $\delta^{44/42}$Ca adakitic sample requires 30% garnet and 70% clinopyroxene (with 28% jadeite) in its residue. Compared to experimental runs of basaltic materials (Fig. S6), 28% jadeite in clinopyroxene indicates a pressure of >2 GPa, which is consistent with the petrogenesis of Dabie low-Mg adakitic granitoids that the depth of crust is >50 km during their emplacement (e.g., Wang et al., 2007; Xiao and Clemens, 2007; He et al., 2011). The protoliths of the sources of low-Mg adakitic rocks may range from pyroxenite-rich cumulates to crystallized basaltic melts, and differences in Al_2O_3 and Na_2O may govern the proportions of garnet and jadeite in clinopyroxene in the residua during partial melting.

5.3. General implications

5.3.1. Implications for the origin of low $\delta^{44/42}$Ca basalts

The role of residual garnet and jadeite-rich clinopyroxene in Ca isotope fractionation may have important implications for the origin of low $\delta^{44/42}$Ca basalts, since garnet and jadeite-rich clinopyroxene are important Ca carrier in pyroxenites and peridotites at high pressures. For example, with increasing pressure, garnet abundance increases and becomes more majoritic, and jadeite proportion in clinopyroxene increases rapidly in the melting residua of MORB-like elogites (e.g., Pertermann and Hirschmann, 2003). Clinopyroxene disappears and garnet becomes the only residual Ca-bearing mineral during partial melting at pressures over 20 GPa (e.g., Thomson et al., 2016). Accordingly, given other parameters constant, partial melts of deeper mantle sources may have lighter Ca isotopic composition. To quantify this effect, experimental data for partial melting of anhydrous MORB-like eclogites at 2–3 GPa (Pertermann and Hirschmann, 2003) and CO_2-bearing subducted oceanic crust at 3–5.1 GPa (Thomson et al., 2016) are applied to a mass balance method modified after Eq. (10). Assuming a source $\delta^{44/42}$Ca of the average terrestrial basalts (0.41, Fig. 2), the calculated partial melts have $\delta^{44/42}$Ca as low as +0.33 at pressure >3.0 GPa (Table S4). Contribution of such low $\delta^{44/42}$Ca melts, either directly or secondarily via hybridization in the sources, may provide an alternative explanation for some low $\delta^{44/42}$Ca OIB-like basalts in previous studies (e.g., Huang et al., 2011; Liu et al., 2017a).

5.3.2. Ca isotopic composition of the upper continental crust

Calcium is a water-soluble element, and large Ca isotope fractionation during Earth surface processes has been observed (e.g., Fantle and Tipper, 2014). Hence, Ca isotopic composition of the upper continental crust cannot be estimated directly using shales and loess. In this study, we estimate Ca isotopic composition of the upper continental crust based on a compilation of updated high precision data of crustal rocks. Following the model of Wedepohl (1995), upper continental crust consists of six major rock units: 25% granites, 20% granodiorites, 5% tonalites, 6% gabbros, 14% sedimentary rocks and 30% metamorphic rocks. Calcium isotopic compositions of the granites,

Table 4
Mass balance model for Ca in the upper continental crust (UCC).

Rock unit	Proportions in the UCC (%)[a]	Average CaO contents (%)[a]	CaO fraction in the UCC (%)	$\delta^{44/42}$Ca	2SE
Sedimentary rocks[b]	14	9.0	30.8	0.33	0.01
Granites[c]	25	1.5	9.2	0.36	0.01
Granodiorites[c]	20	3.83	18.8	0.36	0.01
Tonalites[c]	5	4.9	6.0	0.36	0.01
Gabbros[d]	6	4.58	6.7	0.41	0.01
Metamorphic rocks[e]	30	3.88	28.5	0.36	0.02
UCC				0.35	0.05[f]

[a] Division of rock units, their proportions in the upper continental crust and average CaO contents are from Wedepohl (1995).
[b] Weighted average $\delta^{44/42}$Ca of sedimentary subunits, see detail in Table S5.
[c] Average $\delta^{44/42}$Ca of non-adakitic granitoids in this study and intermediate to felsic samples in previous works (Amini et al., 2009; Simon and DePaolo, 2010; Valdes et al., 2014; Feng et al., 2017; He et al., 2017a; Liu et al., 2017a,b).
[d] Average $\delta^{44/42}$Ca of terrestrial mafic rocks (Huang et al., 2010; Simon and DePaolo, 2010; Huang et al., 2011; Valdes et al., 2014; Jacobson et al., 2015; Feng et al., 2017; He et al., 2017a; Liu et al., 2017a; Zhang et al., 2018; Zhu et al., 2018).
[e] Weighted average $\delta^{44/42}$Ca of metamorphic rocks subunits, see detail in Table S6.
[f] The uncertainty assigned to the estimate of the UCC is calculated based on uncertainties of the Ca isotope composition, proportion and Ca content of each rock unit. The uncertainties of the proportion and Ca content of each rock unit is estimated according to the CaO variation among the existing UCC estimates compiled in Rudnick and Gao (2003) (4.00 ± 0.41 wt.%, 2SE, 95% c.i.), assuming that the proportion and Ca content of each rock unit have the same relative errors.

granodiorites and tonalites are assumed to be the CaO-weighted mean value of non-adakitic granitoids measured in this study and intermediate to felsic samples in previous works (Amini et al., 2009; Simon and DePaolo, 2010; Valdes et al., 2014; Feng et al., 2017; He et al., 2017a; Liu et al., 2017a,b). The gabbro unit is estimated as the mean terrestrial mafic rocks (Huang et al., 2010; Simon and DePaolo, 2010; Huang et al., 2011; Valdes et al., 2014; Jacobson et al., 2015; Feng et al., 2017; He et al., 2017a; Liu et al., 2017a; Zhang et al., 2018; Zhu et al., 2018). The sedimentary unit consists of four subunits: shales, sandstones, mafic volcanics and carbonates. Their $\delta^{44/42}$Ca and CaO content of each subunit are taken from published data (e.g., Fantle and Tipper, 2014; Feng et al., 2017; He et al., 2017a) and the detailed calculations are listed in Table S5. Since Ca isotopes may not fractionate significantly during high-temperature metamorphism (Lu et al., 2017), Ca isotopic compositions of metamorphic rocks are represented by their protoliths (see detail in Table S6). Accordingly, the mean Ca isotopic composition of upper continental crust is estimated to be $\delta^{44/42}Ca = +0.35 \pm 0.05$ (2SE, 95% c.i.) (Table 4), which is lighter than the upper mantle ($+0.46 \pm 0.02$, Kang et al., 2017) by 0.11. This is probably owing to (i) isotopic fractionation caused by removal of mafic cumulates under the arcs (e.g., Lee et al., 2012; Jagoutz and Schmidt, 2013); (ii) isotopic fractionation during run-off due to weathering; and (iii) contribution of sediments including carbonates with low $\delta^{44/42}$Ca.

6. CONCLUSIONS

In order to study Ca isotope fractionation during crustal melting and magma differentiation, we report high-precision Ca isotopic data for Dabie adakitic and non-adakitic granitoids, and hornblende, plagioclase, garnet and clinopyroxene separates.

Hornblende has heavier Ca isotopic composition than its co-existing plagioclase with $\Delta^{44/42}Ca_{hbl-plg}$ of $+0.10 \pm 0.02$ at 663–761 °C. There is significant Ca isotope fractionation between co-existing garnet and clinopyroxene, ranging from $+0.06 \pm 0.03$ to $+0.38 \pm 0.04$. $A_{grt-cpx}$ ($A_{grt-cpx} = \Delta^{44/42}Ca_{grt-cpx} \times T^2/10^6$) decreases with jadeite proportion in clinopyroxene, indicating a clinopyroxene compositional effect on inter-mineral Ca isotope fractionation.

Eight non-adakitic granitoids from the Dabie orogen have homogeneous $\delta^{44/42}$Ca with an average of $+0.37 \pm 0.03$ (2SD, $N = 8$), indicating insignificant Ca isotope fractionation during crustal melting and magma differentiation without garnet involved. Nine Dabie low-Mg adakitic granitoids display a significant $\delta^{44/42}$Ca variation ranging from $+0.24 \pm 0.02$ to $+0.38 \pm 0.02$, which negatively correlates with $(Dy/Yb)_N$. The significant Ca isotope fractionation among low-Mg adakitic granitoids is likely due to the combined control of residual garnet and jadeite-rich clinopyroxene during crustal melting. Thus, this study provides an alternative explanation of low $\delta^{44/42}$Ca basalts by partial melting under higher pressure (e.g., >3 GPa for pyroxenites) where Ca is hosted in garnet and jadeite-rich clinopyroxene. Combined with the literature data, the current best $\delta^{44/42}$Ca estimate of the upper continental crust is $+0.35 \pm 0.05$ (2SE, 95% c.i.).

ACKNOWLEDGEMENT

Constructive reviews from Dr. Luc Doucet, Dr. Ryan D. Mills and one anonymous reviewer and efficient editorial efforts by Dr. Horst Marschall are greatly appreciated. We appreciate Dr. Qiang Wang for providing three low-Mg adakitic samples (EGB-2, YFD-3 and YFD-8) and Dr. Wang-Ye Li for mineral separates of Dabie eclogites. Xunan Meng and Wenning Lu are thanked for the help during sample analysis. This work is supported by the National Key R&D Program of China (2016YFC0600408); the National

Natural Science Foundation of China (41673012, 41688103, 41730214); the Strategic Priority Research Program of the Chinese Academy of Sciences (XDB18030603); the Fundamental Research Funds for the Central Universities (3-7-5-2019-07) and State Key Lab. of Geological Processes and Mineral Resources. This is CUGB petrogeochemical contribution No. PGC-201543.

APPENDIX A. SUPPLEMENTARY MATERIAL

Supplementary data to this article can be found online at https://doi.org/10.1016/j.gca.2019.05.030.

REFERENCES

Allred A. (1961) Electronegativity values from thermochemical data. *J. Inorg. Nucl. Chem.* **17**, 215–221.

Amini M., Eisenhauer A., Böhm F., Holmden C., Kreissig K., Hauff F. and Jochum K. P. (2009) Calcium isotopes ($\delta^{44/40}$Ca) in MPI-DING reference glasses, USGS rock powders and various rocks: Evidence for Ca isotope fractionation in terrestrial silicates. *Geostandards Geoanalytical Res.* **33**, 231–247.

Atherton M. P. and Petford N. (1993) Generation of sodium-rich magmas from newly underplated basaltic crust. *Nature* **362**, 144.

Chang M., Wu H., Li M., Feng J. and He Y. (2014) Study of zircon inclusions of Dabie post-collisional granitoids-contraints on source and melting-depth of adakitic rocks. *Bull. Mineral. Petrol. Geochem.* **33**, 477–483.

Chen Y. J., Wang P., Li N., Yang Y. F. and Pirajno F. (2017) The collision-type porphyry Mo deposits in Dabie Shan, China. *Ore Geol. Rev.* **81**, 405–430.

Defant M. J. and Drummond M. S. (1990) Derivation of some modern arc magmas by melting of young subducted lithosphere. *Nature* **347**, 662.

Dimitrov V. and Komatsu T. (2012) Correlation among electronegativity, cation polarizability, optical basicity and single bond strength of simple oxides. *J. Solid State Chem.* **196**, 574–578.

Fantle M. S. and Tipper E. T. (2014) Calcium isotopes in the global biogeochemical Ca cycle: implications for development of a Ca isotope proxy. *Earth Sci. Rev.* **129**, 148–177.

Farkaš J., Déjeant A., Novák M. and Jacobsen S. B. (2011) Calcium isotope constraints on the uptake and sources of Ca^{2+} in a base-poor forest: a new concept of combining stable ($\delta^{44/42}$Ca) and radiogenic (εCa) signals. *Geochim. Cosmochim. Acta* **75**, 7031–7046.

Feng C., Qin T., Huang S., Wu Z. and Huang F. (2014) First-principles investigations of equilibrium calcium isotope fractionation between clinopyroxene and Ca-doped orthopyroxene. *Geochim. Cosmochim. Acta* **143**, 132–142.

Feng L.-P., Zhou L., Yang L., DePaolo D. J., Tong S.-Y., Liu Y.-S., Owens T. L. and Gao S. (2017) Calcium isotopic compositions of sixteen USGS reference materials. *Geostandards Geoanalytical Res.* **41**, 93–106.

Hawthorne F. C. and Oberti R. (2007) Amphiboles: crystal chemistry. *Rev. Mineral. Geochem.* **67**, 1–54.

He Y., Li S., Hoefs J., Huang F., Liu S.-A. and Hou Z. (2011) Post-collisional granitoids from the Dabie orogen: new evidence for partial melting of a thickened continental crust. *Geochim. Cosmochim. Acta* **75**, 3815–3838.

He Y., Li S., Hoefs J. and Kleinhanns I. C. (2013) Sr–Nd–Pb isotopic compositions of Early Cretaceous granitoids from the Dabie orogen: constraints on the recycled lower continental crust. *Lithos* **156–159**, 204–217.

He Y., Wang Y., Zhu C., Huang S. and Li S. (2017a) Mass-independent and mass-dependent ca isotopic compositions of thirteen geological reference materials measured by thermal ionisation mass spectrometry. *Geostandards Geoanalytical Res.* **41**, 283–302.

He Y., Wu H., Ke S., Liu S.-A. and Wang Q. (2017b) Iron isotopic compositions of adakitic and non-adakitic granitic magmas: Magma compositional control and subtle residual garnet effect. *Geochim. Cosmochim. Acta* **203**, 89–102.

Holland T. and Blundy J. (1994) Non-ideal interactions in calcic amphiboles and their bearing on amphibole-plagioclase thermometry. *Contrib. Miner. Petrol.* **116**, 433–447.

Huang F., Li S., Dong F., He Y. and Chen F. (2008) High-Mg adakitic rocks in the Dabie orogen, central China: implications for foundering mechanism of lower continental crust. *Chem. Geol.* **255**, 1–13.

Huang F., Zhou C., Wang W., Kang J. and Wu Z. (2019) First-principles calculations of equilibrium Ca isotope fractionation: implications for oldhamite formation and evolution of lunar magma ocean. *Earth Planet. Sci. Lett.* **510**, 153–160.

Huang S., Farkaš J. and Jacobsen S. B. (2010) Calcium isotopic fractionation between clinopyroxene and orthopyroxene from mantle peridotites. *Earth Planet. Sci. Lett.* **292**, 337–344.

Huang S., Farkaš J. and Jacobsen S. B. (2011) Stable calcium isotopic compositions of Hawaiian shield lavas: evidence for recycling of ancient marine carbonates into the mantle. *Geochim. Cosmochim. Acta* **75**, 4987–4997.

Huang S., Farkaš J., Yu G., Petaev M. I. and Jacobsen S. B. (2012) Calcium isotopic ratios and rare earth element abundances in refractory inclusions from the Allende CV3 chondrite. *Geochim. Cosmochim. Acta* **77**, 252–265.

Jacobson A. D., Grace Andrews M., Lehn G. O. and Holmden C. (2015) Silicate versus carbonate weathering in Iceland: New insights from Ca isotopes. *Earth Planet. Sci. Lett.* **416**, 132–142.

Jagoutz O. and Schmidt M. W. (2013) The composition of the foundered complement to the continental crust and a re-evaluation of fluxes in arcs. *Earth Planet. Sci. Lett.* **371**, 177–190.

Kang J.-T., Ionov D. A., Liu F., Zhang C.-L., Golovin A. V., Qin L.-P., Zhang Z.-F. and Huang F. (2017) Calcium isotopic fractionation in mantle peridotites by melting and metasomatism and Ca isotope composition of the Bulk Silicate Earth. *Earth Planet. Sci. Lett.* **474**, 128–137.

Kang J.-T., Zhu H.-L., Liu Y.-F., Liu F., Wu F., Hao Y.-T., Zhi X.-C., Zhang Z.-F. and Huang F. (2016) Calcium isotopic composition of mantle xenoliths and minerals from Eastern China. *Geochim. Cosmochim. Acta* **174**, 335–344.

Lee C.-T. A., Luffi P., Chin E. J., Bouchet R., Dasgupta R., Morton D. M., Le Roux V., Yin Q.-Z. and Jin D. (2012) Copper systematics in arc magmas and implications for crust-mantle differentiation. *Science* **336**, 64–68.

Lehn G. O. and Jacobson A. D. (2015) Optimization of a ^{48}Ca–^{43}-Ca double-spike MC-TIMS method for measuring Ca isotope ratios ($\delta^{44/40}$Ca and $\delta^{44/42}$Ca): limitations from filament reservoir mixing. *J. Anal. At. Spectrom.* **30**, 1571–1581.

Li W.-Y., Teng F.-Z., Xiao Y., Gu H.-O., Zha X.-P. and Huang J. (2016) Empirical calibration of the clinopyroxene–garnet magnesium isotope geothermometer and implications. *Contrib. Miner. Petrol.* **171**, 61.

Li W.-Y., Teng F.-Z., Xiao Y. and Huang J. (2011) High-temperature inter-mineral magnesium isotope fractionation in eclogite from the Dabie orogen, China. *Earth Planet. Sci. Lett.* **304**, 224–230.

Liu F., Li X., Wang G., Liu Y., Zhu H., Kang J., Huang F., Sun W., Xia X. and Zhang Z. (2017a) Marine carbonate component in the mantle beneath the southeastern Tibetan plateau:

evidence from magnesium and calcium isotopes. *J. Geophys. Res. Solid Earth* **122**, 9729–9744.
Liu F., Zhu H. L., Li X., Wang G. Q. and Zhang Z. F. (2017b) Calcium isotopic fractionation and compositions of geochemical reference materials. *Geostandards Geoanalytical Res.* **41**, 675–688.
Liu S.-A., Huang J., Liu J., Wörner G., Yang W., Tang Y.-J., Chen Y., Tang L., Zheng J. and Li S. (2015) Copper isotopic composition of the silicate Earth. *Earth Planet. Sci. Lett.* **427**, 95–103.
Liu S.-A., Teng F.-Z., He Y., Ke S. and Li S. (2010) Investigation of magnesium isotope fractionation during granite differentiation: implication for Mg isotopic composition of the continental crust. *Earth Planet. Sci. Lett.* **297**, 646–654.
Lu W., He Y., Ke S. and Li S. (2017) *Behavior of Calcium Isotopes During Slab Subduction*. Goldschmidt Abstracts.
Ma C., Li Z., Ehlers C., Yang K. and Wang R. (1998) A post-collisional magmatic plumbing system: mesozoic granitoid plutons from the Dabieshan high-pressure and ultrahigh-pressure metamorphic zone, east-central China. *Lithos* **45**, 431–456.
Magna T., Gussone N. and Mezger K. (2015) The calcium isotope systematics of Mars. *Earth Planet. Sci. Lett.* **430**, 86–94.
Mills R. D., Simon J. I. and DePaolo D. J. (2018) Calcium and neodymium radiogenic isotopes of igneous rocks: tracing crustal contributions in felsic magmas related to super-eruptions and continental rifting. *Earth Planet. Sci. Lett.* **495**, 242–250.
Morimoto N. (1988) Nomenclature of pyroxenes. *Mineral. Petrol.* **39**, 55–76.
Moyen J.-F. (2009) High Sr/Y and La/Yb ratios: the meaning of the "adakitic signature". *Lithos* **112**, 556–574.
Nesbitt H. W. and Young G. (1982) Early Proterozoic climates and plate motions inferred from major element chemistry of lutites. *Nature* **299**, 715.
Nestola F., Boffa Ballaran T., Liebske C., Thompson R. and Downs R. T. (2008) The effect of the hedenbergitic substitution on the compressibility of jadeite. *Am. Mineral.* **93**, 1005–1013.
Novak G. and Gibbs G. (1971) The crystal chemistry of the silicate garnets. *Am. Mineral.* **56**, 791–825.
Perchuk A. L., Burchard M., Schertl H. P., Maresch W. V., Gerya T. V., Bernhardt H. J. and Vidal O. (2009) Diffusion of divalent cations in garnet: multi-couple experiments. *Contrib. Miner. Petrol.* **157**(5), 573.
Pertermann M. and Hirschmann M. M. (2003) Anhydrous partial melting experiments on MORB-like eclogite: phase relations, phase compositions and mineral–melt partitioning of major elements at 2–3 GPa. *J. Petrol.* **44**, 2173–2201.
Rapp R. P. (1995) Amphibole-out phase boundary in partially melted metabasalt, its control over liquid fraction and composition, and source permeability. *J. Geophys. Res. Solid Earth* **100**, 15601–15610.
Rapp R. P., Shimizu N., Norman M. and Applegate G. (1999) Reaction between slab-derived melts and peridotite in the mantle wedge: experimental constraints at 3.8 GPa. *Chem. Geol.* **160**, 335–356.
Rapp R. P. and Watson E. B. (1995) Dehydration melting of metabasalt at 8–32 kbar: implications for continental growth and crust-mantle recycling. *J. Petrol.* **36**, 891–931.
Richet P., Bottinga Y. and Javoy M. (1977) A review of hydrogen, carbon, nitrogen, oxygen, sulphur, and chlorine stable isotope fractionation among gaseous molecules. *Annu. Rev. Earth Planet. Sci.* **5**, 65–110.
Rudnick R. L. and Gao S. (2003) Composition of the continental crust. *Treatise geochem.* **3**, 659.
Sen C. and Dunn T. (1994) Dehydration melting of a basaltic composition amphibolite at 1.5 and 2.0 GPa: implications for the origin of adakites. *Contrib. Miner. Petrol.* **117**, 394–409.
Shannon R. D. (1976) Revised effective ionic radii and systematic studies of interatomic distances in halides and chalcogenides. *Acta Crystallogr. Sect. A: Crystal Phys., Diffr., Theor. General Crystallogr.* **32**, 751–767.
Simon J. I. and DePaolo D. J. (2010) Stable calcium isotopic composition of meteorites and rocky planets. *Earth Planet. Sci. Lett.* **289**, 457–466.
Simon J. I., DePaolo D. J. and Moynier F. (2009) Calcium isotope composition of meteorites, Earth, and Mars. *Astrophys. J.* **702**, 707–715.
Smyth J. R. and Bish D. L. (1988) *Crystal Structures and Cation Sites of the Rock-Forming Minerals*. Allen & Unwin Boston.
Sun S. s. and McDonough W. F. (1989) Chemical and isotopic systematics of oceanic basalts: implications for mantle composition and processes. *Geol. Soc., London, Spec. Publ.* **42**, 313–345.
Thomson A. R., Walter M. J., Kohn S. C. and Brooker R. A. (2016) Slab melting as a barrier to deep carbon subduction. *Nature* **529**, 76–79.
Valdes M. C., Moreira M., Foriel J. and Moynier F. (2014) The nature of Earth's building blocks as revealed by calcium isotopes. *Earth Planet. Sci. Lett.* **394**, 135–145.
Wang Q., Wyman D. A., Xu J., Jian P., Zhao Z., Li C., Xu W., Ma J. and He B. (2007) Early Cretaceous adakitic granites in the Northern Dabie Complex, central China: implications for partial melting and delamination of thickened lower crust. *Geochim. Cosmochim. Acta* **71**, 2609–2636.
Wang W., Qin T., Zhou C., Huang S., Wu Z. and Huang F. (2017a) Concentration effect on equilibrium fractionation of Mg-Ca isotopes in carbonate minerals: insights from first-principles calculations. *Geochim. Cosmochim. Acta* **208**, 185–197.
Wang W., Zhou C., Qin T., Kang J.-T., Huang S., Wu Z. and Huang F. (2017b) Effect of Ca content on equilibrium Ca isotope fractionation between orthopyroxene and clinopyroxene. *Geochim. Cosmochim. Acta* **219**, 44–56.
Wang Z.-Z., Liu S.-A., Liu J., Huang J., Xiao Y., Chu Z.-Y., Zhao X.-M. and Tang L. (2017c) Zinc isotope fractionation during mantle melting and constraints on the Zn isotope composition of Earth's upper mantle. *Geochim. Cosmochim. Acta* **198**, 151–167.
Wedepohl K. H. (1995) The composition of the continental crust. *Geochim. Cosmochim. Acta* **59**, 1217–1232.
Winther K. T. (1996) An experimentally based model for the origin of tonalitic and trondhjemitic melts. *Chem. Geol.* **127**, 43–59.
Wu H., He Y., Bao L., Zhu C. and Li S. (2017) Mineral composition control on inter-mineral iron isotopic fractionation in granitoids. *Geochim. Cosmochim. Acta* **198**, 208–217.
Xiao L. and Clemens J. D. (2007) Origin of potassic (C-type) adakite magmas: experimental and field constraints. *Lithos* **95**, 399–414.
Xiong X. L., Adam J. and Green T. H. (2005) Rutile stability and rutile/melt HFSE partitioning during partial melting of hydrous basalt: implications for TTG genesis. *Chem. Geol.* **218**, 339–359.
Zhang H., Wang Y., He Y., Teng F.-Z., Jacobsen S. B., Helz R. T., Marsh B. D. and Huang S. (2018) No measurable calcium isotopic fractionation during crystallization of Kilauea Iki lava lake. *Geochem., Geophys., Geosyst.* **19**, 3128–3139.
Zhang X., Ganguly J. and Ito M. (2010) Ca–Mg diffusion in diopside: tracer and chemical inter-diffusion coefficients. *Contrib. Miner. Petrol.* **159**, 175.

Zhao X., Zhang Z., Huang S., Liu Y., Li X. and Zhang H. (2017) Coupled extremely light Ca and Fe isotopes in peridotites. *Geochim. Cosmochim. Acta* **208**, 368–380.

Zhou, C., Wang, W., Kang, J., Wu, Z., Huang, F. (2016) First-principles calculations of equilibrium calcium isotope fractionation among ca-bearing minerals, AGU Fall Meeting Abstracts.

Zhu H., Liu F., Li X., Wang G., Zhang Z. and Sun W. (2018) Calcium isotopic compositions of normal mid-ocean ridge basalts from the Southern Juan De Fuca ridge. *J. Geophys. Res. Solid Earth* **123**, 1303–1313.

Executive editor: Jeffrey G. Catalano